Original Paper

Vibrational spectroscopic investigations of lead borate and lead aluminoborate glasses

Klaus Witke, Ulrike Harder, Manfred Willfahrt, Thomas Hübert and Peter Reich

Bundesanstalt für Materialforschung und -prüfung, Berlin (Germany)

Lead borate (PB) and lead aluminoborate (PBA) glasses in the systems $x\text{PbO} \cdot (100-x)\text{B}_2\text{O}_3$ ($0 \leq x \leq 75$ mol%) and $x\text{PbO} \cdot (95-x)\text{B}_2\text{O}_3$, $5\text{Al}_2\text{O}_3$ ($0 \leq x \leq 80$ mol%), respectively, have been prepared and investigated by Raman and infrared reflectance spectroscopy to obtain qualitative and quantitative information on the structure of glasses. Using the Martin-Brenig model, structural correlation lengths were determinated from boson peak positions of temperature-reduced Raman spectra and transversal sound velocities. Kramers-Kronig analysis was used to transform the measured infrared reflectance spectra into complex dielectric functions. The imaginary part of the complex dielectric function contains the absorption properties of the material. A band separation computer programme has been used to get more detailed information from the spectra. Far infrared and low-frequency Raman spectra contain information about vibrations of the PbO component within the network.

Schwingungsspektroskopische Untersuchungen von Bleiborat- und Bleialumoborat-Gläsern

Bleiborat(PB)- und Bleialumoborat(PBA)-Gläser der Zusammensetzung (Stoffmengenanteil in %): $x\text{PbO} \cdot (100-x)\text{B}_2\text{O}_3$ ($0 \leq x \leq 75$) bzw. $x\text{PbO} \cdot (95-x)\text{B}_2\text{O}_3$, $5\text{Al}_2\text{O}_3$ ($0 \leq x \leq 80$) wurden hergestellt und durch Raman- und Infrarot-Reflexionsspektroskopie untersucht, um qualitative und quantitative Informationen zur Glasstruktur zu erhalten. Aus den Boson-Peakfrequenzen der temperaturreduzierten Raman-Spektren und gemessenen transversalen Schallgeschwindigkeiten wurden über das Martin-Brenig-Modell Strukturkorrelationslängen bestimmt. Mit der Kramers-Kronig-Analyse wurden aus gemessenen IR-Reflexionsspektren komplexe dielektrische Funktionen und aus deren Imaginärteil die Absorptionseigenschaften der Gläser ermittelt. Um detailliertere Informationen zu erhalten, wurde ein Computer-Bandentrennungsprogramm benutzt. FIR- und niederfrequente Raman-Spektren lieferten Informationen über Schwingungen der PbO-Baueinheiten im Glasnetzwerk.

1. Introduction

Lead oxide is an interesting component of borate glasses because PbO can enter the glass both as a network modifier and as a network former. The extreme difference between the masses of boron and lead atoms leads to a separation of vibrational modes of the borate network and of the PbO polyhedra and favours spectroscopic investigations. On the other hand, the large mass of the lead atom results in very low-lying fundamental vibrations of the PbO polyhedra and in overlapping with boson peaks of the low-frequency Raman spectra.

Raman spectroscopic studies in the frequency range above 500 cm^{-1} have been carried out on PB glasses for PbO contents varying between 22 and 85 mol% [1 to 3]. In addition to high frequencies, the low-frequency range of glasses with PbO concentrations (x) below 20 mol% were investigated, which are opaque as a result of liquid phase separation. Quantitative results were obtained concerning the content of boroxol and borate rings [4 and 5]. Furthermore, structural aspects of specific glasses with 25, 33.3, 50 and 75 mol% PbO are studied [6 and 7]. The present paper extends the structural studies to glasses containing 5 mol% Al_2O_3, because they do not show visible liquid phase separation and, thus, allow the recording of Raman spectra in the boson peak region because of their optical transparency.

The majority of infrared investigations of glasses in the past were based on transmittance measurements. Powdered glass samples were dispersed in KBr or other matrix materials. But the influence of the matrix material can lead to distortions of the line shapes of the IR bands. The extent of these distortions depends on the dielectric properties of the matrix material and on the particle size of the glass powder. For this reason, IR reflectance spectroscopy on compact samples seems to be a better method for investigations of glasses. Kramers-Kronig analysis makes it possible to calculate the true value of the dielectric function of a material from its IR reflectance spectrum. Infrared reflectance measurements in the mid and far infrared region were carried out on lithium borate glasses [8] and alkali diborate glasses [9]. Results of far infrared transmittance measurements of lead borate glasses have been published [10]. IR and Raman spectra of some lead borate glasses containing 20 mol% Cr_2O_3 besides up to 10 mol% of Al_2O_3 have been analyzed [11].

IR reflectance spectra of lead borate glasses were measured in the mid infrared region (4000 to 400 cm^{-1}) to get information about the content of structural borate

Received August 21, revised manuscript November 13, 1995.

groups as a function of the PbO concentration. Measurements in the far infrared region (400 to 20 cm^{-1}) help to understand the structural role of Pb^{2+} cations within the glass network.

2. Experimental

2.1 Glass preparation

Glasses were prepared from chemically pure (p.a.) reagents, H_3BO_3, Pb_3O_4, and Al_2O_3, which were melted in a platinum crucible for 30 min at 800 to 1200 °C depending on chemical composition. The melt was pressed between steel plates and, after annealing, was cooled down to room temperature. Pieces with the dimensions $(3 \times 3 \times 0.2)$ cm^3 were cut with a diamond cutting disk and polished with boron carbide and diamond powder with particle sizes of 7 and 2.4 µm for the infrared studies.

2.2 Spectroscopic measurements

Raman spectra were recorded with a DILOR XY spectrometer (DILOR, Bensheim (Germany)), equipped with a nitrogen-cooled CCD camera (CCD = Charge-Coupled Device) as a detector. Samples were excited using the 514.5 nm line from a Carl Zeiss ILA 120 argon ion laser (Carl Zeiss Jena (Germany)) with power levels up to 80 mW incident into the entrance optics. Back scattering geometry was used for irregularly formed glassy pieces to record spectra inclusive their low-frequency parts. The vv polarization scattering arrangement supplies spectra of full intensity of all Raman active modes, while the hv one spectra of relative low intensity of polarized bands. In the case of high B_2O_3 content glasses, fresh fracture surfaces were used to exclude recording spectra of boric acid built by hydrolysis.

The infrared measurements were carried out on the BRUKER IFS66v spectrometer (Bruker, Karlsruhe (Germany)), equipped with the far infrared option. A reflectance attachment with variable angle of incidence (θ = 20° to 80°) and polarizers for the mid and far IR were used. An angle of 20° and the direction of polarization perpendicular to the plane of incidence were selected.

The mid infrared spectrum and four spectra segments of the far infrared spectrum were measured separately by using a KBr beam splitter for the mid infrared region and four Mylar beam splitters of various thicknesses (6, 12, 23 and 50 µm) for the far infrared region. The five spectra were merged into one reflectance spectrum containing the whole infrared region from 4000 to 20 cm^{-1}.

Transverse sound velocities were measured using the ultrasonic pulse echo overlap method (a) and the impulse excitation technique (b). For measurements by method (a), each sample had a pair of end faces that are flat and mutually parallel and the dimensions were $(40 \times 20 \times 10)$ mm^3. Ultrasonic travel time was measured at frequencies of 50 and 80 Hz and a temperature of 298 K. For use of method (b), dimensions of the glassy pieces were like those of method (a), but the faces were not ground and polished. The procedure consists of exciting the test object by means of a light external mechanical impulse and of analyzing the transient natural vibration during the subsequent free relaxation. A device type MK5 "Industrial" of the company Grindo Sonic, St. Louis (USA), was used to measure the elastic constants from which the sound velocities were calculated according to the Hooke's law.

2.3 Computer calculations

The IR reflectance measurements are followed by some computer calculations, which are carried out by means of the FSOS software system [12].

The complex dielectric function

$$\hat{\varepsilon}(\tilde{\nu}) = \varepsilon'(\tilde{\nu}) + i\varepsilon''(\tilde{\nu}) \tag{1}$$

includes all optic and dielectric properties of a material. It can be calculated from the complex reflectivity $\hat{r}(\tilde{\nu})$ by solving the inverse Fresnel equations. For radiation polarized perpendicular to the plane of incidence the inverse Fresnel equations result in the following expression:

$$\hat{\varepsilon}_2 = \varepsilon_1' \left\{ \sin^2 \theta_1 + \cos^2 \theta_1 \left[\frac{1 - \hat{r}_\perp}{1 + \hat{r}_\perp} \right]^2 \right\} \tag{2}$$

with $\hat{\varepsilon}_2$ = complex dielectric function of the second medium (glass), ε_1' = dielectric constant of the first medium (air), independent of the wavelengths, θ_1 = angle of incidence, $\hat{r}_\perp$ = perpendicular component of the complex reflectivity $\hat{r}(\tilde{\nu})$.

The complex reflectivity $\hat{r}(\tilde{\nu})$ is defined as

$$\hat{r}(\tilde{\nu}) = (R(\tilde{\nu}))^{1/2} \cdot e^{i\varphi(\tilde{\nu})} \tag{3}$$

where $R(\tilde{\nu})$ is the amount of reflectivity and $\varphi(\tilde{\nu})$ is the phase angle difference between reflected and incident wave.

$\varphi(\tilde{\nu})$ is commonly calculated from the amount of reflectivity $R(\tilde{\nu})$ using the classical Kramers-Kronig transformation according to the equation

$$\varphi(\nu_0) = \frac{2\nu_0}{\pi} \int_0^\infty \frac{\ln(R(\nu))^{1/2}}{\nu^2 - \nu_n^2} \, d\nu \,. \tag{4}$$

The physical equivalent Peterson-Knight transformation

$$\varphi(\nu_0) = \frac{2}{\pi} \int_0^\infty dt \sin \nu_0 t \int_0^\infty \ln(R(\nu))^{1/2} \cos \nu t \, d\nu \tag{5}$$

is used within the FSOS system instead of equation (4).

In the present case the reflectivity $R(\tilde{\nu})$ is known from the reflectance spectrum and the dielectric function $\hat{\varepsilon}(\tilde{\nu})$ has to be calculated. The first step is the calculation of the phase angle difference spectrum $\varphi(\tilde{\nu})$ according to equation (5). After that the complex reflectivity $\hat{r}(\tilde{\nu})$ is known (equation (3)). Equation (2) is used to calculate the dielectric function $\hat{\varepsilon}_2(\tilde{\nu})$ of the glass.

The absorption coefficient spectra $\alpha(\tilde{\nu})$ are calculated from the dielectric functions $\hat{\varepsilon}_2(\tilde{\nu})$ as follows:

$$\alpha(\tilde{\nu}) = 4\pi\,\tilde{\nu} \cdot \mathrm{Im}(\sqrt{\hat{\varepsilon}_2})\,. \tag{6}$$

A band separation computer programme (part of the OPUS package of the BRUKER company) is used to obtain quantitative results. All of the absorption coefficient spectra are separated into 11 to 13 bands (sums of Gaussian and Lorentzian functions) within the frequency region 20 to 2000 cm^{-1}. Each of the calculated bands is represented by wave number position, maximum absorption coefficient, bandwidth, integral and bandshape.

3. Results

The Raman spectra of the investigated PBA glasses are given in figure 1. They are very similar to those of the PB glasses [5]. Spectra of glasses containing up to 20 mol% PbO are dominated by a sharp strong band at 805 cm^{-1}, shifting its position towards lower wave numbers and decreasing in intensity with increasing content of PbO. On the contrary, a shoulder/band at $\approx$770 cm^{-1} grows in intensity by the same measure. The intensity ratio I_{770}/I_{805} is lower than that for the PB glasses. While the inversion of that intensity ratio occurs below 25 mol% PbO for the PB glasses, it takes place above 25 mol% PbO for the PBA glasses. A linear relationship exists between the logarithm of that intensity ratio and the oxide content, x_{MO}, for PB glasses [5] and other binary borate glasses [13]. For PBA glasses, the relationship

$$\ln(I_{770}/I_{805}) = \ln(Q) = 0.112\,x_{PbO} - 3.112 \tag{7}$$

results from 16 measured intensity ratios of six glasses with different PbO contents from 5 up to 30 mol% with a standard deviation of 0.011 and a correlation coefficient of 0.994.

The addition of Al_2O_3 to the system $PbO-B_2O_3$ avoids visible liquid phase separation or crystallization of melts for PbO contents below 20 mol% and allows to obtain optical transparent glasses. Vibrational spectra do not directly indicate the presence of AlO_4 units by separate bands; however, differences between the spectra of PB and PBA glasses may be attributed to the effect of the AlO_4 units on the formation and connection of BO_3 and BO_4 groups, respectively.

The region of the spectra between 1150 and 1500 cm^{-1} shows a broad, unresolved band of considerable relative intensity. Band maxima change their position and relative intensity with increasing lead oxide content. This points to the fact that Raman bands under each envelope must be assigned to different borate groups.

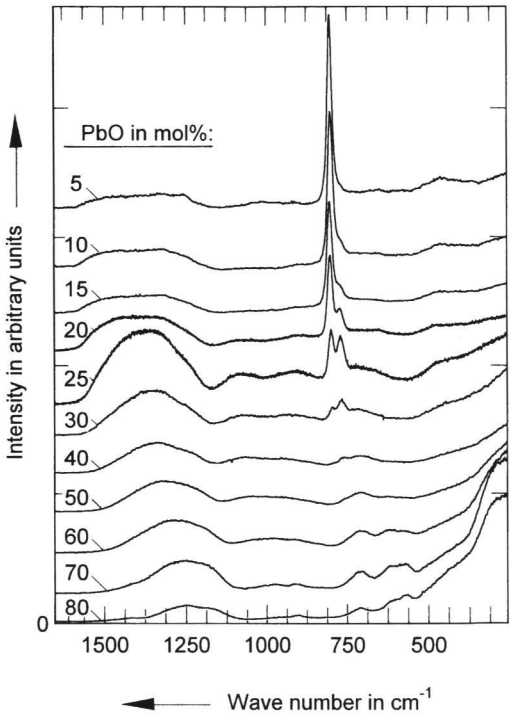

Figure 1. Raman spectra (vv-polarized) of PBA glasses.

The range below 200 cm^{-1} of the hv-polarized spectra is presented in the temperature-reduced form. Reduction was done assuming that $C_b \sim \omega$, where C_b is the coupling coefficient, and ω the Raman frequency [14]: $I(T) = I(\omega)/[1 + n(\omega)]$, $n(\omega) = [\exp(h\,c\,\tilde{\nu}/(k\,T)) - 1]^{-1}$; T = 300 K (h = Planck's constant, c = speed of light, k = Boltzmann's constant; figure 2). As a result of this reduction, very low-lying peaks slightly shift their position to higher wave numbers. Excepting the vitreous B_2O_3 and the glasses containing more than 50 mol% PbO, the rest of the spectra show one broad asymmetric band only, the boson peak, whose position increases from 27 cm^{-1} for B_2O_3 to 51 cm^{-1} for the 40 mol% PbO glass and decreases again to 33 cm^{-1} for the 80 mol% PbO glass. A second band develops in the high-frequency wing of the boson peak from a weak shoulder at about 80 cm^{-1} for the 20 mol% PbO glass into a broad plateau from $\approx$40 to $\approx$130 cm^{-1} for the 60 mol% PbO glass and splits up into a very strong band at 135 and a weaker one at $\approx$80 cm^{-1} for the investigated glass with the highest PbO content. Contrary to the boson peak, these bands are polarized and have a higher relative intensity in the vv-polarized spectra. Recording in a hv-polarized scattering arrangement was chosen in order to reduce their relative intensity and, thus, to reduce their influence on the position of the bo-

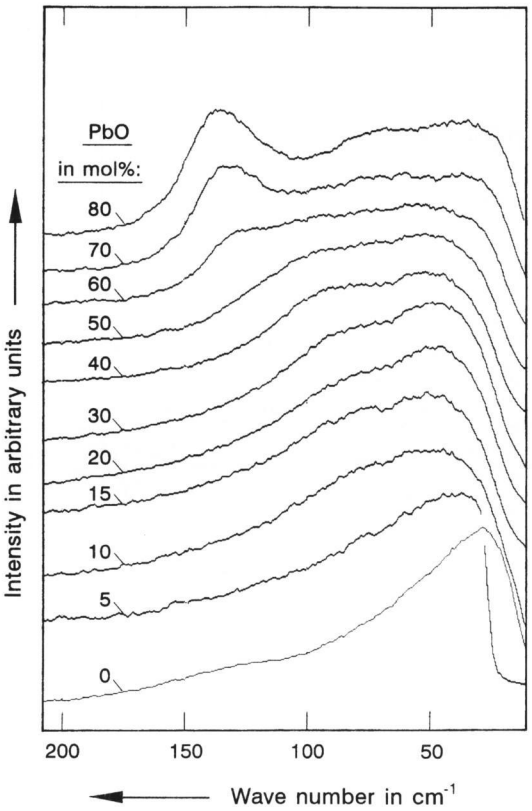

Figure 2. Temperature-reduced hv-polarized low-frequency Raman spectra of PBA glasses (0 mol% PbO glass without Al_2O_3).

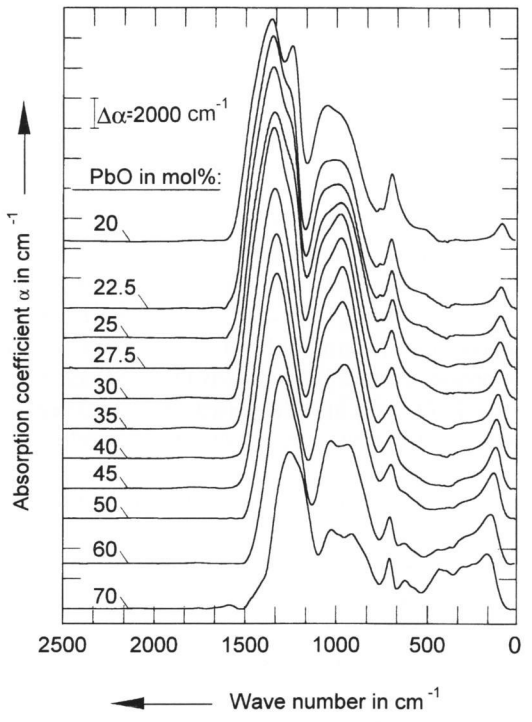

Figure 3. IR absorption coefficient spectra of PB glasses calculated by Kramers-Kronig analysis from reflectance spectra.

son peak (compare hv-polarized spectrum, figure 2, and vv-polarized one (figure 7) of the 80 mol% PbO PBA glass).

The absorption coefficient spectra of PB and PBA glasses (figures 3 and 4) are the results of computer calculations from infrared reflectance spectra measured with perpendicularly polarized radiation by an incident angle of 20° using software package FSOS (see section 2.3 and [12]). Absorption coefficient spectra determined in this way are comparable to absorbance spectra measured by means of transmission technique (e.g. spectra of thin glassy films or of powder probes dispersed in KBr). Figure 5 shows a typical example of a band separation.

Nearly all known crystalline borate compounds show a strong band between 1300 and 1390 cm^{-1}. PB and PBA glasses with PbO contents between 20 and 70 mol% absorb also very strongly in this region. The band shifts towards lower wave numbers with rising amounts of PbO. Another band appears between 1240 and 1260 cm^{-1}, mostly as a shoulder. Its position shifts from 1240 to 1190 cm^{-1} with increasing PbO contents of the glasses. In PBA glasses its intensity remains nearly constant. In PB glasses the intensity of this band or shoulder decreases for PbO contents between 20 and 40 mol% and rises again between 50 and 70 mol% PbO.

The spectra of all PB and PBA glasses measured show two strongly overlapping bands at about 950 and 1050 cm^{-1}. The band at 950 cm^{-1} grows in intensity with increasing amounts of PbO up to 40 mol%. For higher PbO contents it decreases again. The band at 1050 cm^{-1} seems to remain nearly constant for all compositions (in mol%) from $x = 20$ to $x = 50$. It attains its maximum for $x = 60$ and is less intensive again for $x = 70$.

In the far infrared region an asymmetric band at about 100 cm^{-1} is found, which shifts towards higher wave numbers with increasing PbO content, whereas bandwidth and absorption coefficients of this band are increasing (figures 3 and 4). For PbO contents higher than 50 mol% an additional band occurs at about 300 cm^{-1}. Also for glasses with high PbO contents, another band develops between 400 and 500 cm^{-1}.

4. Discussion

4.1 Size of scattering units

Low-frequency Raman spectra are the subject of an increasing number of papers concerned with the investigation of the structure of non-crystalline solids. As the vibrational frequency tends towards zero, the competition between the decreasing density of vibrational states and the increasing thermal population results in the so-called "boson" peak [15] dominating in intensity the low-frequency part of the spectra. The Martin-Brenig (M-B) elastic continuum model relates the position of the boson peak, ω_m, of the temperature-reduced

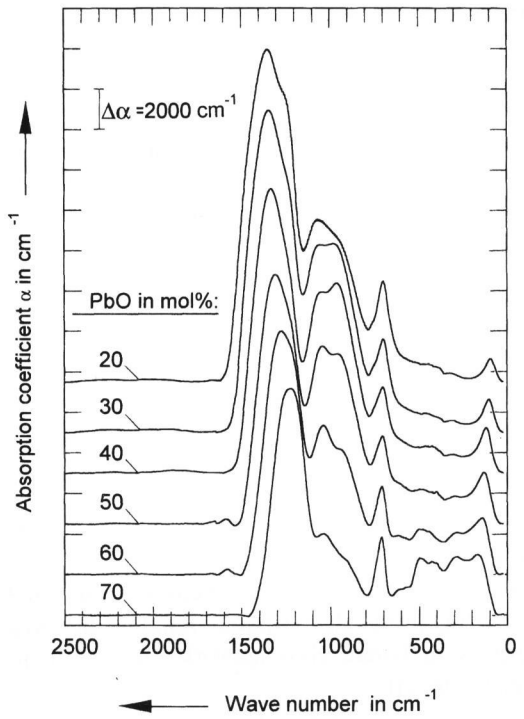

Figure 4. IR absorption coefficient spectra of PBA glasses obtained by Kramers-Kronig analysis from reflectance spectra.

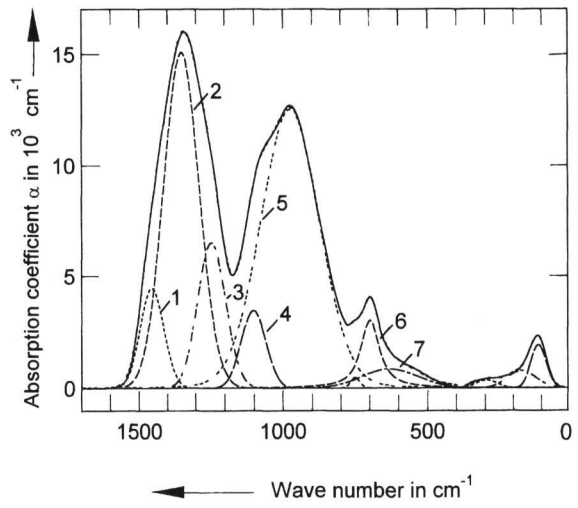

Figure 5. Band separation of the absorption coefficient spectrum of the 35 mol% PbO PB glasses. Peaks 1 to 7 correspond to IR bands no. 1 to 7 in table 1.

Raman spectra and the transversal sound velocity, v_{tr}, to the size of the ordered regions, the Structural Correlation Lengths (SCL), R_c [16]:

$$R_c = \frac{v_{tr}}{\pi \omega_m c}, \tag{8}$$

The M-B model provides a direct explanation for the universal presence of a low-frequency Raman peak for oxide glasses and was also attributed to a maximum in the Raman coupling coefficient, which is related to the SCL in the glass [13 and 17]. The universality of the shape of the boson peak was observed for inorganic glasses independent of their chemical composition [14]. On the basis of the M-B model, the boson peak of alkali and thallium borate glasses has been analyzed [18].

Experimentally determined transversal sound velocities, boson peak positions and SCL values of both PB and PBA glasses calculated by equation (8) are shown in figures 6a to c. Sound velocities show a relative maximum for a PbO content of about 25mol%, which is somewhat broader for the PBA glass. A maximum at the same position also exists for the dependence of the SCL on composition, and broader for the PBA glass. Obviously, sound velocities of low PbO content glasses are dominated by SCL. The behaviour corresponds to the alkali borate glasses [18] with similar sizes of the cation (Na^+, K^+): SCL values decrease with increasing PbO content as a result of increasing sound velocities. However, the behaviour of the SCL values of glasses with PbO contents > 60 mol% is contrary to that of the sound velocities. While sound velocities decrease monotonously above 30 mol% PbO, SCL values show a relative minimum at 60 mol% PbO and increase again with higher PbO contents. Together with the growing intensity of peaks which correspond to the tetragonal crystalline PbO, the increasing SCL values reflect the growing role of PbO as a network former. Such a role of PbO also is seen as a result of neutron scattering investigations [19].

4.2 Identification of structural units

4.2.1 PbO_x species

It is instructive to establish somewhat like a degree of order as the ratio of SCL values to the dimensions of the molecular structural units. Thus, the diameter of the BO_3 unit is 0.25 nm and that of the six-membered boroxol ring as a main structure unit of vitreous B_2O_3 is 0.56 nm [18]. Tetragonal PbO forms a layer structure of square-based pyramids with the lead atom at the apex and the lead atoms lying alternately above and below the plane of oxygen atoms. The base and the edge length of a PbO_4 pyramid are 0.23 and 0.28 nm, respectively [20]. Taking into consideration the existence of structural units larger than a boroxol ring like di- or triborate groups for medium PbO contents [1 to 3], the degree of order of glasses containing more than 70 mol% PbO is higher even than that of pure B_2O_3. There is maximal randomness in the 60 mol% PbO glasses. The Raman spectrum of that glass shows first indications of peaks at ≈ 80 and ≈130 cm^{-1}. From 60 mol% upwards, PbO takes the dominating role as a glass former, and the resulting network structure should be similar to that of tetragonal

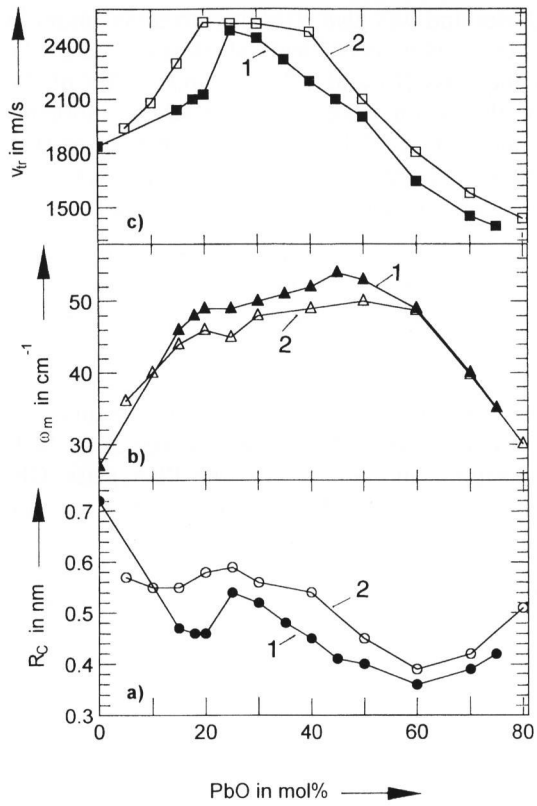

Figures 6a to c. Structure correlation length R_c (figure a), boson band position ω_m (figure b) and transversal sound velocity v_{tr} (figure c) of PB (curve 1) and PBA (curve 2) glasses.

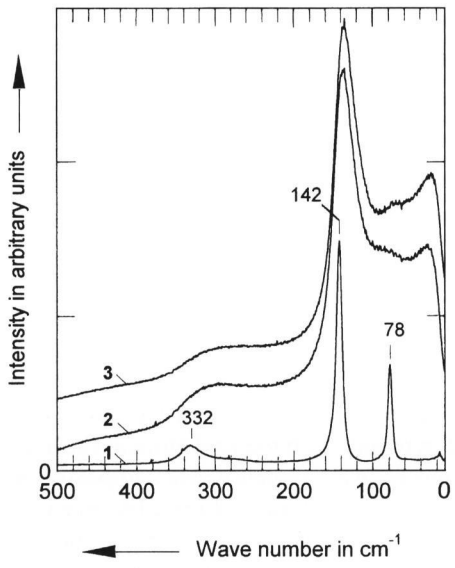

Figure 7. vv-polarized Raman spectra. Curve 1: tetragonal crystalline PbO, curve 2: 75 mol% PbO PB glass, curve 3: 80 mol% PbO PBA glass.

PbO. Figure 7 shows the vv-polarized spectra of the PB and PBA glasses with the highest PbO contents, respectively, in comparison with that of tetragonal crystalline PbO, the bands of which have been assigned to A_{1g} (78), B_{1g} (142) and E_g (36 and 332 cm^{-1}) fundamental vibrations [20]. The formation of PbO_4 pyramids in lead borate glasses containing high PbO contents is known from NMR investigations [21], however, these results do not allow the distinction between tetragonal and orthorhombic pyramids.

The band in the infrared reflection spectra near 300 cm^{-1} corresponds to the band at 290 cm^{-1} (A_{2u} + E_u) found for tetragonal PbO. Besides this band, due to covalent Pb–O bonds, another type of Pb–O bonds gives IR absorption bands between 100 and 200 cm^{-1}. Because of its lower wave number, this band is assigned to ionic Pb–O bonds. It is interpreted to come from motions of Pb^{2+} cations in the borate glass network.

Figures 3 and 4 show that wave number position and intensity of the Pb^{2+} cation vibrational band are strongly influenced by the PbO content of the glass. Both wave number and intensity increase with rising amount of PbO in the glass. Cation vibrations of alkali metal cations in borate glass networks have been investigated [22 to 24].

The cations are surrounded by negatively charged non-bridging oxygen ions, which are found at breaking-off sites of the glass network. It has been shown that the characteristic frequency, $\tilde{\nu}$, of a cation vibration in a network [23] is given by

$$\tilde{\nu}^2 = \left[\frac{A}{48\pi^3 c^2 \varepsilon_0}\right] \frac{q_C q_A}{\mu r_0^3} \left[\frac{r_0}{\varrho} - 2\right] \tag{9}$$

where q_C and q_A are the charge of cation and anionic site, respectively, c is the speed of light, ε_0 the permittivity of free space, ϱ the repulsion parameter in the Born-Mayer potential, and A a pseudo-Madelung constant. The reduced mass of the vibration, μ, and the equilibrium cation–oxygen distance, r_0, depend on the site geometry which includes the coordination number of the cation, Z.

The cation vibrational band shows an asymmetric band profile for PB and PBA glasses. It can be separated into two Gaussian bands at different wave number positions (figure 5). The wave numbers of both bands, $\tilde{\nu}_1^2$ and $\tilde{\nu}_2^2$, increase systematically with rising part of PbO in the glass. The squares of wave numbers of the two calculated cation bands are plotted versus the molar concentrations of PbO in the glass in figures 8a and b. The error bars base on an estimated uncertainty of band position of 5 cm^{-1}. The dependence is linear over wide concentration ranges. The deviation of the measured points from the calculated line is higher in the case of PB glasses.

For a specific type of cation, changes of the vibrational frequency, $\tilde{\nu}$, can be caused by changes of the charge of the anionic site, q_A, and/or by changes of the site geometry. Assuming that reduced mass, μ, and equilibrium cation–oxygen distance, r_0, remain constant, the

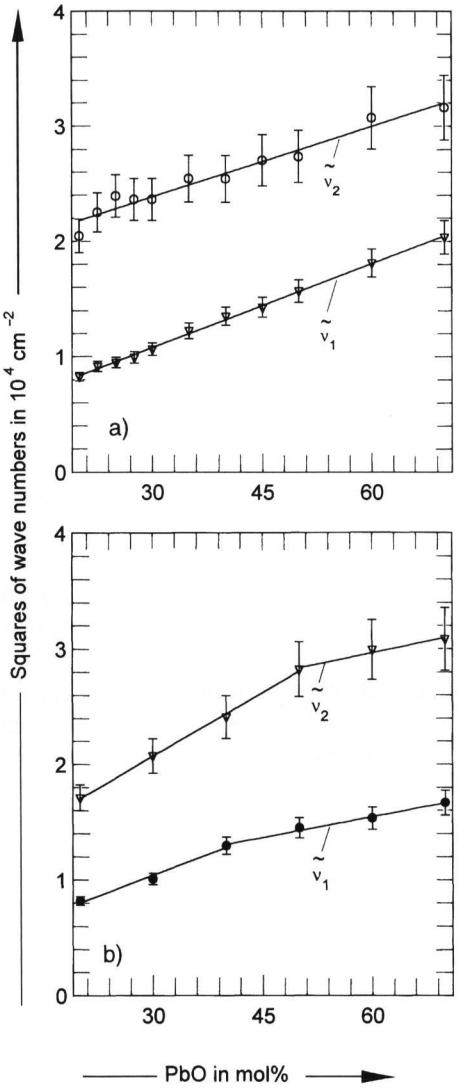

Figures 8a and b. Squares of wave numbers of Pb^{2+} cation vibrations versus lead oxide concentration of a) PB glasses, b) PBA glasses.

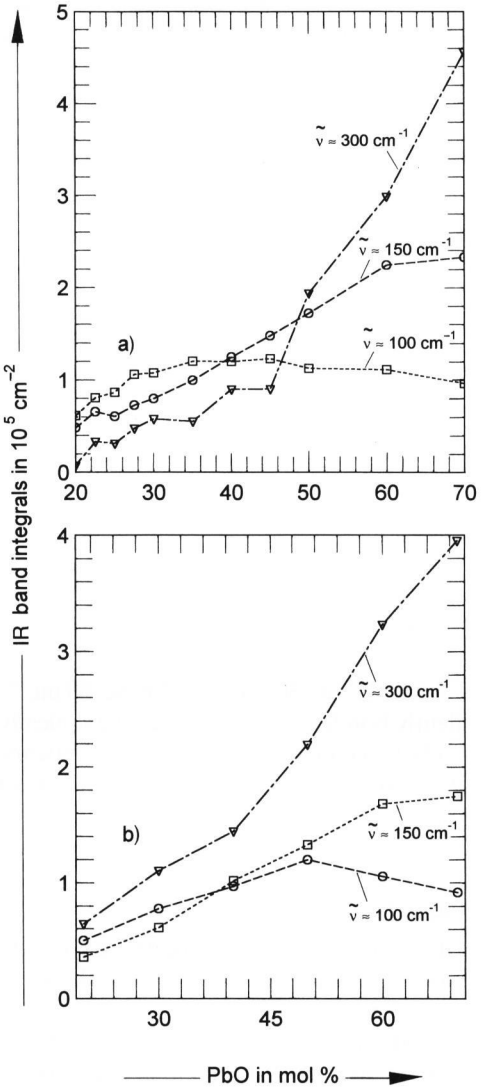

Figures 9a and b. IR band integrals of the far infrared bands versus lead oxide concentration of a) PB glasses, b) PBA glasses.

linear rise of $\tilde{\nu}^2$ is due to the linear increase of the anionic charge density of the network sites. On the other hand, it has been shown for alkali metal borate glasses that cation–oxygen distances, reduced masses and the Madelung constant vary with the coordination number of the cation. An increase of the cation motion frequency with coordination number was found for all alkali metal cations [23]. Thus, an increase of the coordination numbers of the cations could also contribute to the shift of the cation bands to higher wave numbers observed with increasing PbO contents (figures 8a and b).

The curves in figure 8b which describe the dependence of the squares of the wave numbers of the cation bands from the PbO contents of the PBA glasses show a little change in slope at 40 and 50 mol%, respectively. This change in slope is not found for PB glasses (figure 8a). It may have several origins and shall not be further discussed here.

igures 9a and b present the integral intensities of the three Pb–O vibrational bands at about 300, 150 and 100 cm^{-1} versus the amount of PbO in the glass. The relative error of the band areas used as measure of intensity amounts to about 20 %. (Error bars would make the figures less clear. For this reason they were not included.) The intensity of the cation band of higher wave number (150 cm^{-1}) is continuously increasing, but the other band (100 cm^{-1}) becomes more intensive up to 40 mol% PbO (PB glasses) or 50 mol% PbO (PBA glasses) and decreases again for higher PbO contents. The band at about 300 cm^{-1} is relatively small up to 45 mol% and grows very fast at PbO contents above 45 mol%. These results correspond to those of Raman spectra. For very low PbO content, lead oxide predominantly acts as modifier (ionic Pb–O bond, bands at 100 and 150 cm^{-1}). With increasing PbO content, it behaves as network modifier as well as glass former (covalent

Table 1. Assignment of bands of the mid infrared spectra to vibrations of borate groups

IR band no.	wave numbers in lead borate glass spectra in cm^{-1}	band position in crystalline alkali borates [8] in cm^{-1}	assignment
1	1410 to 1475	1440 to 1445	pentaborate groups, metaborate chains, pyroborate units
2	1290 to 1360	1300 to 1390	pentaborate, triborate and diborate groups, pyroborate and orthoborate units
3	1190 to 1240	1240 to 1260	boroxol rings, pentaborate and triborate groups, metaborate chains and orthoborate units, pyroborate units (weak)
4	1040 to 1100	1100 to 1125	pentaborate and triborate groups, pyroborate units
5	920 to 975	980 to 990	diborate and triborate groups
		900 to 950	diborate groups, pentaborate groups (weak)
6	725 to 770 690 to 705	700 to 775	bending vibrations of various borate units
7	550 to 630	590 to 650	bending vibrations of the isolated BO_3^{3-} ion

Pb–O bonds, band at ca. 300 cm^{-1}). Above 50 mol% PbO, the covalently bonded lead dominates the ionically bonded part. PbO becomes the dominating network former in comparison to B_2O_3 above 60 mol% PbO (Raman spectra).

4.2.2 BO_x species

The interpretation of the infrared spectra of borate glasses was based on the comparison with those of crystalline borate compounds of known structure, according to the model of Krogh-Moe [25] and with the spectrum of pure vitreous B_2O_3 [27], which is known to consist of boroxol rings. A series of IR absorption coefficient spectra was published of carefully prepared and measured crystalline lithium borates [8]. The region of 1200 to 1500 cm^{-1} is assigned to asymmetric stretching vibrations of trigonal BO_3 units. Asymmetric stretching vibrations of tetrahedral BO_4 lead to absorption in the 850 to 1200 cm^{-1} region. The bands of bending vibrations of various borate segments are found around 700 cm^{-1}. In the mid infrared region, the IR absorption coefficient spectra of PB and PBA glasses (figures 3 and 4) are quite similar to absorbance or absorption coefficient spectra of alkali and alkaline earth borate glasses measured by other authors [8, 24 to 28]. The spectra of PB as well as of PBA glasses show three broad bands in the 1200 to 1500 cm^{-1}, the 850 to 1200 cm^{-1} region and around 700 cm^{-1}. The band between 400 and 500 cm^{-1} is due to librational motions of isolated BO_3 groups [10] and is also present in the spectrum of lithium orthoborate [8].

The wave number positions of the bands of the mid infrared PB and PBA glass spectra calculated by band separation are compared with those of the corresponding bands in the spectra of crystalline alkali borates [8] in table 1. The interpretation is added in the last column. The wave numbers of all bands in the spectra of crystalline alkali borates are on average somewhat higher than in those of lead borate glasses. The reason for this difference is that the borate groups become more and more isolated by the successive addition of amounts of PbO to the glass. The result of isolation of a structural group is the shift of the IR band to lower wave numbers [27]. On the other hand, the wave number difference may also be the effect of different cations.

Table 1 shows that only the band between 920 and 975 cm^{-1} is characteristic for diborate and triborate groups. (Pentaborate groups are ignored because of the relatively low intensity of the band in the spectrum of the crystalline pentaborate). All the other bands represent at least three different structure elements. A band between 1240 and 1260 cm^{-1} is present in the spectra of crystalline triborate, pentaborate, metaborate, pyroborate and orthoborate [8] and pure vitreous B_2O_3 [29], but not in the spectra of diborate [8]. The spectra of crystalline diborate and triborate compounds contain a particularly strong band between 980 and 990 cm^{-1}, whereas another strong band between 1100 and 1125 cm^{-1} appears in the spectra of crystalline pentaborate, triborate and pyroborate compounds. For this reason it is not possible to identify the structural elements of the glasses in dependence of composition completely by means of infrared measurements only. But nevertheless, some conclusions can be drawn which have to be understood more as hypothesis than as proved facts.

It has been recognized that the structures of PB and PBA glasses depend in a similar manner on the lead oxide content. Structural changes become evident more clearly in PB glasses. On the other hand, the behaviour of PBA glasses with changing composition is more balanced, which is expressed also by the more flat maximum of the SCL values for the 10 to 40 mol% PbO

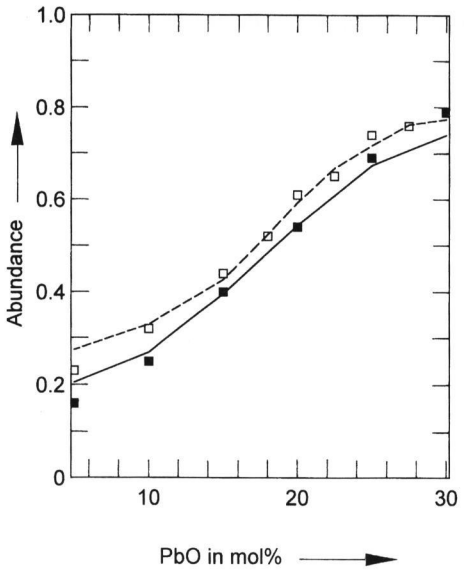

Figure 10. Relative content of borate rings versus lead oxide concentration for PB (□) and PBA (■) glasses.

glasses (figure 6). The relative intensity of the two bands around 1000 cm^{-1} is higher for PB glasses. That means that the fraction of boron atoms with fourfold coordination is higher in PB glasses.

4.3 Quantitative estimation of structural units

A difference of the PBA to the PB glasses consists in the slower growth of the intensity ratio $Q = I_{770}/I_{805}$ with increasing PbO content. Taking into account the assignment of the 805 cm^{-1} peak to the ring vibration of the six-membered boroxol ring and of the 770 cm^{-1} peak to borate rings with one or two BO_4 units [30], that indicates a delayed transformation of boroxol into borate ring structures and, thereby, of BO_3 into BO_4 units. The presence of Al_2O_3 obviously stabilizes boroxol ring structures in the glass network. Raman intensities allow a quantitative estimation of the influence of alumina on that transformation. The relative scattering cross-section, Q_0, has been determinated to be 0.41 ± 0.02 for PB glasses [4]. That value of Q_0 corresponds to the value of Q for equal concentrations of borate and boroxol rings in the glass network. These structural units are also the main constituents in PBA glasses with PbO contents below 30 mol%.

Assuming that the Raman cross-sections of the breathing modes of both boroxol and borate rings are not influenced in a different manner by the presence of Al_2O_3 in the network, the value of Q_0 is transferable to PBA glasses. Then, the relative content of borate rings, c_{B4}, may be calculated by the relationship $c_{B4} = Q/(Q_0 + Q)$ [4 and 5]. Figure 10 illustrates how much lower the relative portion of borate rings is in PBA glasses in comparison to PB glasses. (The contents of boroxol rings equal the difference $1 - c_{Bx}$, respectively. The error of c_{B4} mainly is given by uncertainty of Q_0 and corresponds to the dimension of used symbols in figure 10.) The content of borate rings in the PB glasses corresponds well to N_4 fractions of BO_4 units obtained by ^{11}B-NMR measurements [21]. Theoretical contents of borate rings can be calculated from NMR results assuming that one or two BO_4 units are incorporated into the borate ring. As expected, comparison shows that the Raman spectroscopically determined borate ring contents both for PB [5] and PBA glasses lie close to contents of borate rings containing one BO_4 unit for lower lead oxide concentrations and near to the content of rings containing two BO_4 units for higher ones.

The integrated intensities of the IR bands above 800 cm^{-1} are plotted in figure 11a for the PB and in figure 11b for the PBA glasses versus PbO content. The estimation of error made for figures 9a and b shall apply to these figures. The numbers of the curves correspond to the numbers of bands in table 1. The sum of all band integrals decreases in these diagrams because of the decreasing content of B_2O_3 within the glass. The maximum concentration of di- and triborates is found at 35 to 40 mol% PbO for PB glasses and at 30 mol% PbO for PBA glasses (curve 5 in figures 11a and b). Diborates and triborates show quite similar IR spectra and cannot be easily separated from each other in borate glasses.

Curve 2 shows its maximum at 20 mol% PbO (PBA glasses) and 25 mol% PbO (PB glasses), respectively. Because di- and triborate groups have their maximum concentration at higher PbO contents and pyro- and orthoborate units were never found in borate glasses at such low concentrations of the network modifier component, this maximum represents mainly pentaborate groups. The concentration of pentaborate groups decreases with further addition of PbO. From 30 to 60 mol% PbO di- and triborate contribute to the intensity of band 2. The saddle point at 50 mol% PbO marks the creation of pyro- and / or orthoborate units. Curve 3 represents all borate compounds except of diborate groups. In the case of PB glasses a little maximum is found at 20 mol%, which could be due to boroxol rings. It is known from Raman investigations [2] that boroxol rings exist up to 30 mol% PbO. Above 50 mol% PbO a significant rise of the curve is observed. This change in slope is probably due to the formation of pyro- and/or orthoborate groups, which also corresponds to the behaviour of curve 2. In the spectra of PBA glasses band no. 3 remains nearly constant over the whole concentration range.

Curve 1 decreases continuously with increasing lead oxide concentration. The relatively high intensity for 20 mol% PbO derives from pentaborate groups. The concentration of pentaborates becomes smaller for higher PbO contents. Metaborate chains and pyroborate groups seem to arise only in relatively low concentrations because no rise of curve 1 can be noticed. For lead concentrations above 60 mol% PbO the band at 1450 cm^{-1} nearly disappears. At this lead oxide concentration

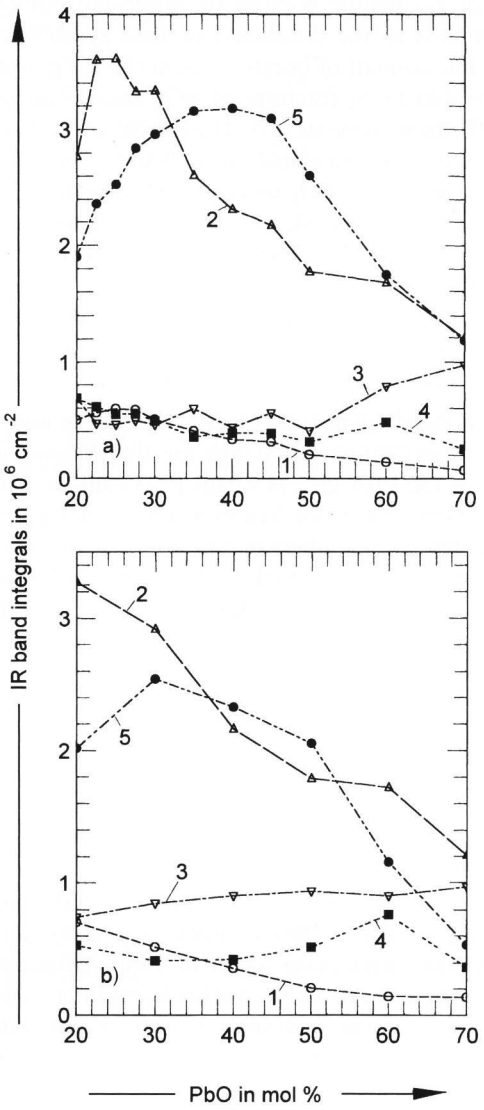

Figures 11a and b. IR band integrals of borate structural units versus lead oxide concentration (IR bands no. 1 to 5 in table 1) of a) PB glasses, b) PBA glasses.

boron probably exists mainly in the form of orthoborate units which do not absorb at 1450 cm^{-1}.

5. Conclusions

The discussion of vibrational spectra using model calculations leads to qualitative and partially quantitative structural information on lead borate and lead aluminoborate glasses.

Using the Martin-Brenig model, structural correlation lengths were determined from boson peak positions of the temperature-reduced Raman spectra and the macroscopic transversal sound velocities. These structural correlation lengths give information on the "middle-range order" of glasses.

Low-frequency Raman and far infrared spectra contain information about vibrations of the PbO component within the network. From 60 mol% upwards, PbO takes the dominating role as a former of the glass network structure, which should be similar to that of tetragonal PbO.

The interpretation of the mid infrared spectra was founded on the comparison with those of crystalline borate compounds of known structure according to the model of Krogh-Moe [25] and with the spectrum of pure vitreous B_2O_3 [26] which is known to consist of boroxol rings.

6. Symbols

A	pseudo-Madelung constant
A_{1g}, B_{1g}, E_g, A_{2u}, E_u	symbols of symmetry types of vibrations
c	speed of light in cm/s
c_{B4}	relative content of borate rings
c_{Bx}	relative content of boroxol rings
C_b	coupling coefficient
h	Planck's constant in J s
hv	electric vectors of incident and scattered light perpendicular to each other
I_i, I_j	intensity of a Raman band of the wave number i and j, respectively
i	imaginary number
k	Boltzmann's constant in J/K
$n(\omega)$	$[\exp(hc\tilde{\nu}/(kT))-1]^{-1}$
Q	relative Raman intensity ratio I_i/I_j
Q_0	relative scattering cross-section
q_A	charge of anionic site
q_C	charge of cation site
$R(\tilde{\nu})$	amount of reflectivity
R_c	structural correlation lengths (SCL) in nm
r_0	equilibrium cation–oxygen distance
$\hat{r}(\tilde{\nu})$	complex reflectivity
$\hat{r}_\perp$	perpendicular component of the complex reflectivity $\hat{r}(\tilde{\nu})$
T	temperature in K
t	time in s
v_{tr}	transversal sound velocity (in nm/s for the calculation of R_c)
vv	electric vectors of incident and scattered light parallel to each other
x_{MO}	content of metal oxide in mol%
Z	coordination number of the cation
$\alpha(\tilde{\nu})$	absorption coefficient spectra
$\hat{\varepsilon}(\tilde{\nu})$	complex dielectric function
$\varepsilon'(\tilde{\nu})$	real part of dielectric function
$\varepsilon''(\tilde{\nu})$	imaginary part of dielectric function
ε_0	permittivity of free space
ε_1'	dielectric constant of the first medium (air), independent of the wavelengths
$\hat{\varepsilon}_2(\tilde{\nu})$	complex dielectric function of the second medium (glass)
θ_1	angle of incidence
μ	reduced mass
ν	frequency in Hz
$\tilde{\nu}$	wave number in cm^{-1}
ϱ	repulsion parameter in the Born-Mayer potential
$\varphi(\tilde{\nu})$	phase angle difference between reflected and incident wave
ω	Raman wave number in the temperature-reduced spectra in cm^{-1}
ω_m	wave number of the boson peak of the temperature-reduced Raman spectra in cm^{-1}

Financial help from the Deutsche Forschungsgemeinschaft and the Fond der Chemischen Industrie is gratefully acknowledged.

7. References

[1] Meera, B. N.; Sood, A. K.; Chandrabhas, N. et al.: Raman study of lead borate glasses. J. Non-Cryst. Solids **126** (1990) p. 224–230.

[2] Meera, B. N.; Ramakrishna, J.: Raman spectral studies of borate glasses. J. Non-Cryst. Solids **159** (1993) p. 1–21.

[3] Zahra, A.-M.; Zahra, C. Y.; Piriou, B.: DSC and Raman studies of lead borate and lead silicate glasses. J. Non-Cryst. Solids **155** (1993) p. 45–55.

[4] Witke, K.; Hübert, T.; Reich, P. et al.: Raman spectroscopic determination of boroxol and borate ring contents in lead borate glasses. J. Raman Spectrosc. **24** (1993) p. 407–410.

[5] Witke, K.; Hübert, T.; Reich, P. et al.: Quantitative Raman investigations of the structure of glasses in the system B_2O_3–PbO. Phys. Chem. Glasses **35** (1994) no. 1, p. 28–33.

[6] Konijnendijk, W. L.; Verweij, H.: Structural aspects of vitreous PbO · $2B_2O_3$ studied by Raman scattering. J. Am. Ceram. Soc. **59** (1976) no. 9–10, p. 459–461.

[7] Akasaka, Y.; Yasui, I.; Nanba, T.: Network structure of RO · $2B_2O_3$ glasses. Phys. Chem. Glasses **34** (1993) no. 6, p. 232–237.

[8] Kamitsos, E. I.; Patsis, A. P.; Karakassides, M. A. et al.: Infrared reflectance spectra of lithium borate glasses. J. Non-Cryst. Solids **126** (1990) p. 52–67.

[9] Kamitsos, E. I.; Patsis, A. P.; Chryssikos, G. D.: Infrared reflectance investigation of alkali diborate glasses. J. Non-Cryst. Solids **152** (1993) p. 246–257.

[10] Tarte, P.; Pottier, M. J.: Far infrared spectrum of lead borate glasses: evidence for the simultaneous occurrence of ionic and covalent Pb–O bonds. In: Gaskell, P. H. (ed.): The structure of non-crystalline materials. Proc. symposium, Cambridge (UK) 1976. London: Taylor & Francis 1977. p. 227–230.

[11] Ram, S.; Ram, K.: IR and Raman studies and effect of γ radiation on crystallization of some lead borate glasses containing Al_2O_3. J. Mater. Sci. **23** (1988) p. 4541–4546.

[12] Hopfe, V.; Korte, E. H.; Klobes, P. et al.: Optical data of rough-surfaced ceramics: Infrared specular and diffuse reflectance versus spectra simulation. Appl. Spectrosc. **47** (1993) p. 423–429.

[13] Soppe, W.: Structure and dynamics of borate glasses. Rijksuniversiteit Groningen (The Netherlands), thesis 1989. p. 54.

[14] Malinovsky, V. K.; Sokolov, A. P.: The nature of Boson peak in Raman scattering in glasses. Solid State Commun. **57** (1986) p. 757–761.

[15] Shuker, R. H.; Gammon, R. W.: Raman-scattering selection-role breaking and the density of states in amorphous materials. Phys. Rev. Lett. **25** (1970) p. 222–225.

[16] Martin, A. J.; Brenig, W.: Model for Brillouin scattering in amorphous solids. Phys. Status Solidi (b) **63** (1974) p. 163–172.

[17] Soppe, W.; Ebens, W.; Hartog, H. W. den: Low-frequency Raman spectroscopy of alkali borate glasses. J. Non-Cryst. Solids **105** (1988) p. 251–257.

[18] Lorösch, J.; Couzi, M.; Pelous, J. et al.: Brillouin and Raman scattering study of borate glasses. J. Non-Cryst. Solids **69** (1984) p. 1–25.

[19] Vedishcheva, N. M.; Shakhmatkin, B. A.; Wright, A. C. et al.: A combined thermodynamic and neutron scattering investigation of glasses in the system PbO–B_2O_3. In: XVI International Congress on Glass, Madrid (Spain) 1992. Vol. 3 p. 41–46. (Bol. Soc. Esp. Ceram. Vid. 31-C (1992) 3.)

[20] Donaldson, J. D.; Donoghue, M. T.; Ross, S. D.: The vibrational spectra of tetragonal and orthohombic PbO. Spectrochim. Acta **30A** (1975) p. 1967–1975.

[21] Bray, P. J.; Leventhal, M.; Hooper, H. O.: Nuclear magnetic resonance investigations of the structure of lead borate glasses. Phys. Chem. Glasses **4** (1963) no. 2, p. 47–66.

[22] Kamitsos. E. I.; Chryssikos, G. D.; Karakassides, M. A.: Vibrational spectra of magnesium-sodium-borate glasses. Pt. 1. Far-infrared investigation of cation–site interactions. J. Phys. Chem. **91** (1987) p. 1067–1073.

[23] Kamitsos, E. I.: Modifying role of alkali-metal cations in borate glass networks. J. Phys. Chem. **93** (1989) p. 1604–1611.

[24] Liu, Changle; Angell, C. A.: Mid- and far-infrared absorption of alkali borate glasses and the limit of superionic conductivity. J. Chem. Phys. **93** (1990) p. 7378–7386.

[25] Krogh-Moe, J.: Interpretation of the infra-red spectra of boron oxide and alkali borate glasses. Phys. Chem. Glasses **6** (1965) no. 2, p. 46–54.

[26] Tarte, P.: The determination of cation co-ordination in glasses by infra-red spectroscopy. In: Prins, J. A. (ed.): Physics of non-crystalline solids. Proc. Int. Conf., Delft (The Netherlands) 1964. Amsterdam: North-Holland Publ. Co. 1965. p. 549–565.

[27] Borrelli, N. F.; McSwain, B. D.; Gouq-Jen Su: The infrared spectra of vitreous boron oxide and sodium borate glasses. Phys. Chem. Glasses **4** (1963) no. 1, p. 11–21.

[28] Kamitsos, E. I.; Karakassides, M. A.; Chryssikos, G. D.: Vibrational spectra of magnesium-sodium-borate glasses. Pt. 2. Raman and mid-infrared investigation of the network structure. J. Phys. Chem. **91** (1987) p. 1073–1079.

[29] Galeener, F. L.; Lucovsky, G.; Mikkelsen, J. C. jr.: Vibrational spectra and the structure of pure vitreous B_2O_3. Phys. Rev. **B 22** (1980) p. 3983–3990.

[30] Bril, T. W.: Raman spectroscopy of crystalline and vitreous borates. Philips Res. Rep. Suppl. (1976) no. 2, p. 243–357.

Address of the authors:
K. Witke, U. Harder, M. Willfahrt, T. Hübert, P. Reich
Bundesanstalt für Materialforschung und -prüfung
Laboratorium VIII. 24
Zweiggelände Berlin-Adlershof
Rudower Chaussee 5, D-12489 Berlin